X-ray

Generation, properties, applications

Miklós Kellermayer

The mysterious X-ray

Wilhelm Konrad Röntgen (1845-1923) Nobel prize, 1901

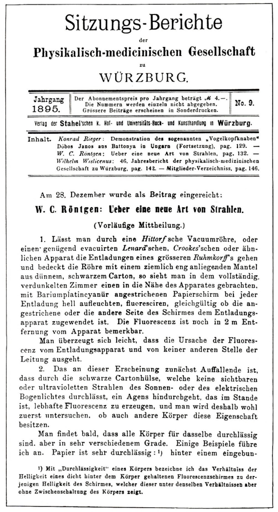

Sitzungs-Berichte
der
Physikalisch-medicinischen Gesellschaft
zu
WÜRZBURG.

Jahrgang 1895.	Der Abonnementspreis pro Jahrgang beträgt ℳ 4.–. Die Nummern werden einzeln nicht abgegeben. Grössere Beiträge erscheinen in Sonderdrucken.	No. 9.

Verlag der **Stahel**'schen k. Hof- und Universitäts-Buch- und Kunsthandlung in **Würzburg.**

Inhalt. *Konrad Rieger*: Demonstration des sogenannten „Vogelkopfknaben" Dóbos Janos aus Battonya in Ungarn (Fortsetzung), pag. 129. — *W. C. Röntgen*: Ueber eine neue Art von Strahlen, pag. 132. — *Wilhelm Wislicenus*: 46. Jahresbericht der physikalisch-medizinischen Gesellschaft zu Würzburg, pag. 142. — Mitglieder-Verzeichniss, pag. 146.

Am 28. Dezember wurde als Beitrag eingereicht:

W. C. Röntgen: Ueber eine neue Art von Strahlen.

(Vorläufige Mittheilung.)

1. Lässt man durch eine *Hittorf*'sche Vacuumröhre, oder einen genügend evacuirten *Lenard*'schen, *Crookes*'schen oder ähnlichen Apparat die Entladungen eines grösseren *Ruhmkorff*'s gehen und bedeckt die Röhre mit einem ziemlich eng anliegenden Mantel aus dünnem, schwarzem Carton, so sieht man in dem vollständig verdunkelten Zimmer einen in die Nähe des Apparates gebrachten, mit Bariumplatincyanür angestrichenen Papierschirm bei jeder Entladung hell aufleuchten, fluoresciren, gleichgültig ob die angestrichene oder die andere Seite des Schirmes dem Entladungsapparat zugewendet ist. Die Fluorescenz ist noch in 2 m Entfernung vom Apparat bemerkbar.

Man überzeugt sich leicht, dass die Ursache der Fluorescenz vom Entladungsapparat und von keiner anderen Stelle der Leitung ausgeht.

2. Das an dieser Erscheinung zunächst Auffallende ist, dass durch die schwarze Cartonhülse, welche keine sichtbaren oder ultravioletten Strahlen des Sonnen- oder des elektrischen Bogenlichtes durchlässt, ein Agens hindurchgeht, das im Stande ist, lebhafte Fluorescenz zu erzeugen, und man wird deshalb wohl zuerst untersuchen, ob auch andere Körper diese Eigenschaft besitzen.

Man findet bald, dass alle Körper für dasselbe durchlässig sind, aber in sehr verschiedenem Grade. Einige Beispiele führe ich an. Papier ist sehr durchlässig:[1]) hinter einem eingebun-

[1]) Mit „Durchlässigkeit" eines Körpers bezeichne ich das Verhältniss der Helligkeit eines dicht hinter dem Körper gehaltenen Fluorescenzschirmes zu derjenigen Helligkeit des Schirmes, welcher dieser unter denselben Verhältnissen aber ohne Zwischenschaltung des Körpers zeigt.

Hand mit Ringen (Hand with Ring): Wilhelm Röntgen's first "medical" X-ray, of his wife's, Anna Bertha Ludwig's hand, taken on 22 December 1895 and presented to Professor Ludwig Zehnder of the Physik Institut (University of Freiburg, 1 January 1896).

Glorious history of x-ray

Transparency – paper funnel radioscope

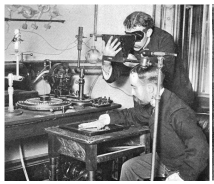

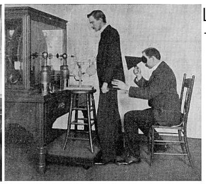

Late 1890s

World war I.

Everyday applications

Shie-fitting fluoroscope (1930-50)

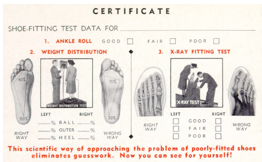

Airport security

Medical applications

1940

1950

Today

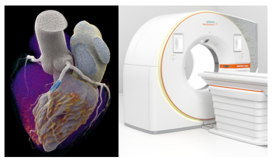

Photon-counting CT

X-rays are electromagnetic waves

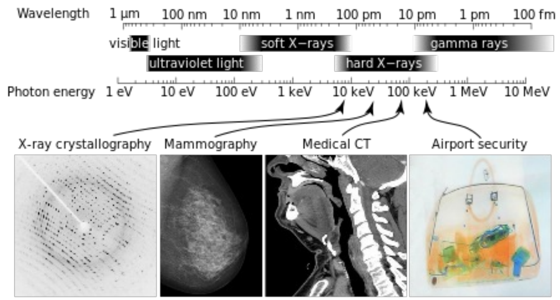

Wavelength 10 - 0.01 nm.
Frequency 30x10^{15} - 30x10^{18} Hz (petaherz - exahertz).
Energy 120 eV - 120 keV.

Generation of X-ray

Non-conventional method

Triboluminescence: light emission evoked by scratching or rubbing. (Francis Bacon, 1605)

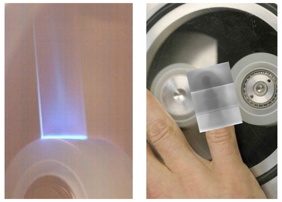

Peeling away sticky tape emits light and X-rays. (Nature News, October 2008)

Usual method: x-ray tube

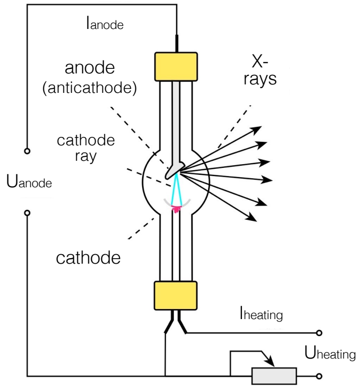

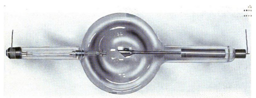

Coolidge x-ray tube (1900s). Heated cathode on the left, anode target on the right. x-ray emitted downwards.

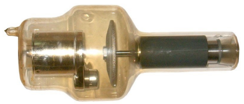

Rotating-anode X-ray tube. Anode rotation is used for cooling.

Mechanism I. “Bremsstrahlung”

Electrons ***decelerate***, thereby loose their kinetic energy, when interacting with the atoms of the anode (“braking radiation”).

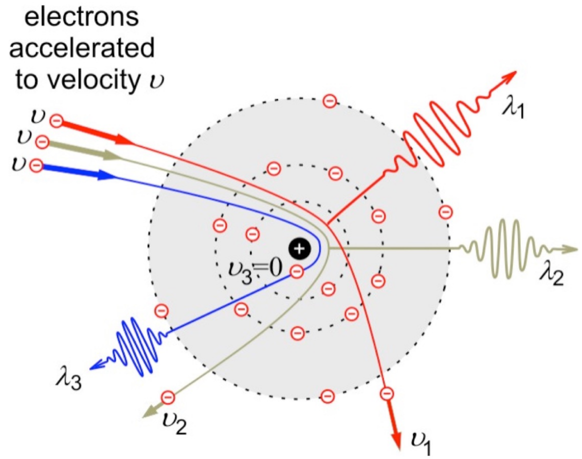

Spectrum of Bremsstrahlung

Continuous

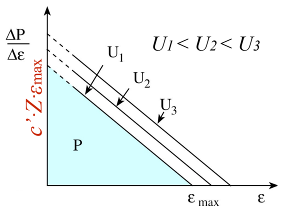

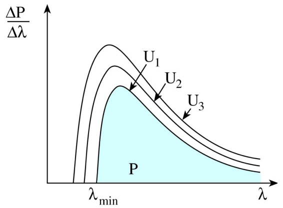

$$eU_{anode} = \varepsilon_{max} = hf_{max}$$

Maximal photon energy (ε_{max})
N.B.: Total kinetic energy of electron is transformed in one step (rare event).
e: electron's charge;
U_{anode}: accelerating voltage;
eU_{anode}: acceleration work;
h: Planck's constant;
f_{max}: limiting frequency

$$\lambda_{min} = \frac{hc}{e} \cdot \frac{1}{U_{anode}}$$

Limiting wavelength (λ_{min})
(Duane-Hunt Law)
N.B.: Limiting wavelength is inversely proportional to accelerating voltage.
c: light speed;
hc/e: constant (1.2398 kV·nm)

$$\frac{\Delta P}{\Delta \varepsilon} = c' \cdot Z \cdot (\varepsilon_{max} - \varepsilon)$$

Energy spectrum
(energy dependence of power)

$$P_{tot} = \frac{1}{2} c' \cdot Z \cdot \varepsilon_{max}^2 = c \cdot Z \cdot U_{anode}^2 \cdot e^2$$

$$P_{tot} = C_{Rtg} \cdot I_{anode} \cdot U_{anode}^2 \cdot Z$$

Total power (P_{tot})
(based on the area of the triangle)
C_{Rtg}: coefficient (1.1x10^{-9} V^{-1});
I_{anode}: anode current (number of electrons hitting the anode per unit time);
Z: atomic number of the anode atoms

$$\eta = \frac{P_{tot}}{P_{in}} = \frac{C_{Rtg} \cdot I_{anode} \cdot U_{anode}^2 \cdot Z}{I_{anode} \cdot U_{anode}} = C_{Rtg} \cdot U_{anode} \cdot Z$$

Efficiency (η)
P_{in}: invested power
N.B.: Typically, η < 1%.

Mechanism II. Characteristic X-ray

Knocked-out inner-shell electron is replaced by one on a higher-energy shell

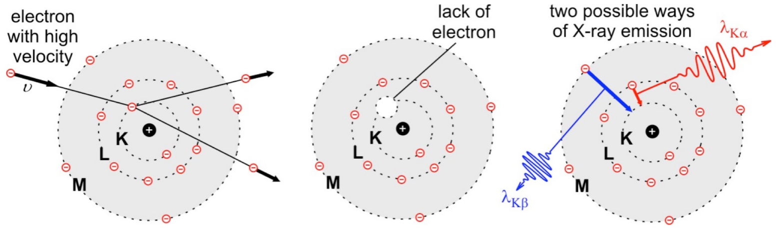

Spectrum of characteristic X-ray

Linear

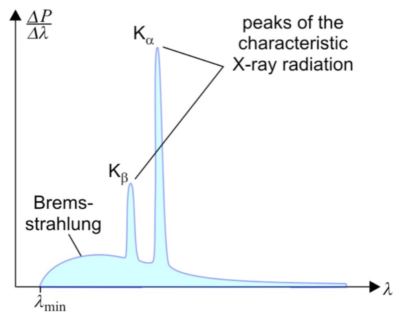

X-ray spectrum characterizes *atomic* composition

Because inner-shell electrons participate in characteristic X-radiation, only the ***atomic*** (and not the molecular) properties are revealed

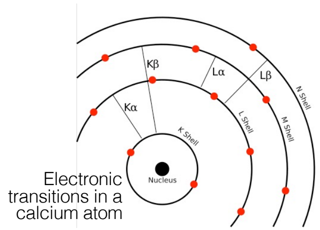

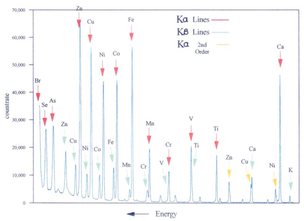

Energy dispersive X-ray fluorescence spectrum

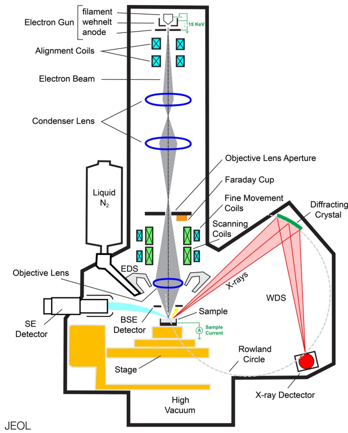

X-ray spectroscope (in an electron microscope!) (measures x-ray energy spectrum)

Interaction of x-ray with matter

1. Diffraction

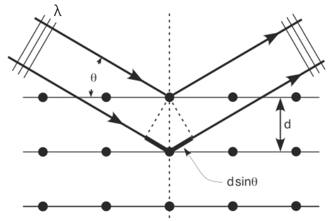

Condition of constructive interference: $2d\sin\theta = n\lambda$

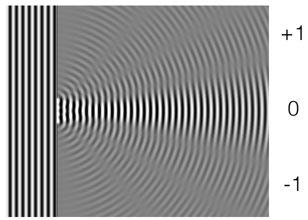

2. Absorption

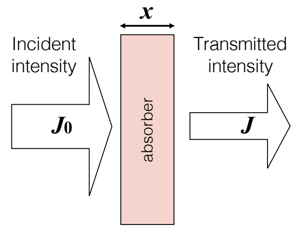

Exponential **attenuation** principle

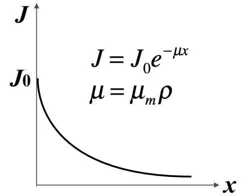

$$J = J_0 e^{-\mu x}$$

$$\mu = \mu_m \rho$$

μ : linear attenuation coefficient
μ_m : mass attenuation coefficient (cm^2/g)
ρ : density (g/cm^3)

Attenuation mechanisms

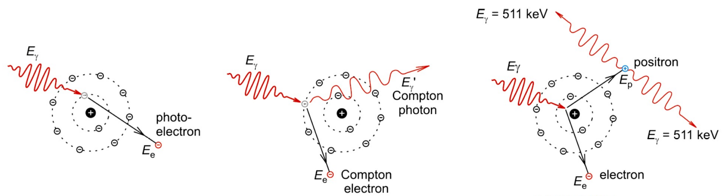

a.) photoeffect
$E_\gamma = A + E_e$
A = work function (escape energy)

b.) Compton scattering
$E_\gamma = A + E_e + E_\gamma'$

c.) pair production, annihilation
$E_\gamma = 2 m_e c^2 + E_e + E_p$
(if $E_\gamma > 1022$ keV)

$$\tau = \tau_m \rho \qquad \sigma = \sigma_m \rho \qquad \kappa = \kappa_m \rho$$

τ_m, σ_m, κ_m: mass attenuation coefficients, ρ: density

$$\mu_m = \tau_m + \sigma_m + \kappa_m$$

Mechanism	Photon energy (ε) dependence of the mass attenuation coefficient	Atomic number (Z) dependence of the mass attenuation coefficient	Relevant energy range in soft tissue
Photoeffect	$\sim 1/\varepsilon^3$	$\sim Z^3$	10 - 100 keV
Compton scatter	falls gradually with ε	~Z/A (A: mass number)	0.5 - 5 MeV
Pair production	rises slowly with ε	$\sim Z^2$	> 5 MeV

Diagnostic X-ray:
1. Contrast mechanism between soft tissue and bone: photoeffect ($\sim Z^3$)
2. Contrast mechanism within soft tissue: Compton-scatter ($\sim\rho$)

Photoeffect attenuation depends strongly on photon energy and atomic number

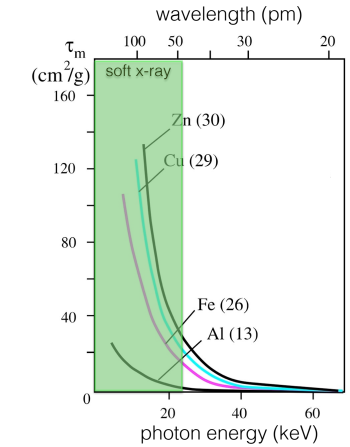

$$\tau_m = const \cdot \frac{Z^3}{\varepsilon^3} = C \cdot \lambda^3 \cdot Z^3$$

For multi-component system: "effective atomic number" (Z_{eff})

$$Z_{eff} = \sqrt[3]{\sum_{i=1}^{n} w_i Z_i^3}$$

ε=photon energy
Z=atomic number
w=mole fraction
n=number of components

Material	Z_{eff}
Air	7.3
Water	7.7
Soft tissue	7.4
Bone	13.8

Application I. X-ray imaging

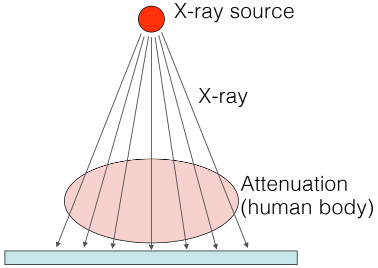

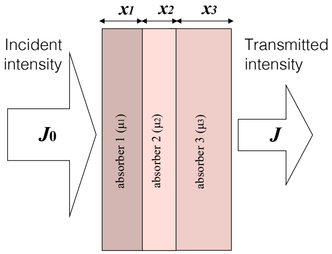

$$J = J_0 e^{-(\mu_1 x_1 + \mu_2 x_2 + \mu_3 x_3 + ...)}$$

$$\lg \frac{J_0}{J} = (\mu_1 x_1 + \mu_2 x_2 + \mu_3 x_3 + ...) \cdot \lg e$$

μ_n : n[th] absorber's attenuation coefficient

x_n : n[th] absorber's thickness

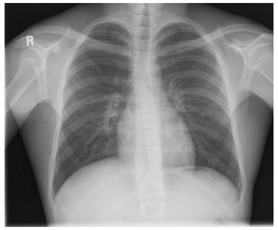

The X-ray image is a **summation image** ("X-ray image", "radiographic image", "roentgenogram"). Contrast arises due to spatially varying attenuation.

Improving X-ray imaging I.

Increasing contrast: contrast agents

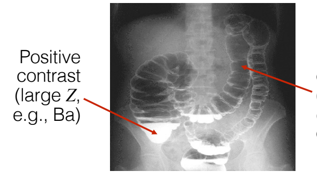

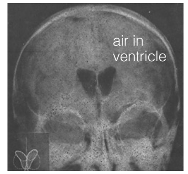

Enhancing sensitivity: intensifier

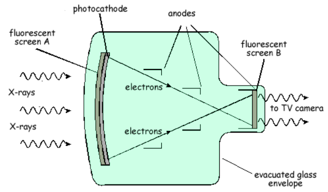

Background subtraction: "Digital Subtraction Angiography" (DSA)

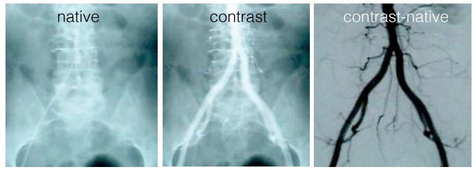

Improving X-ray imaging II. Spatial resolution

Bi-directional X-ray imaging

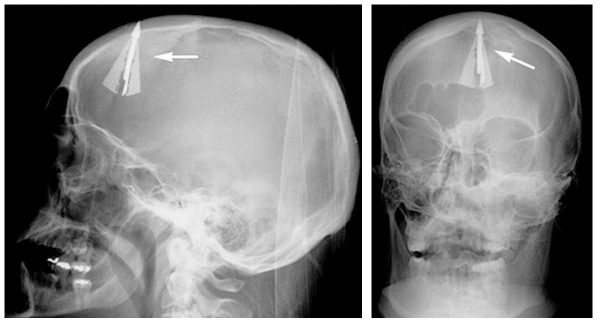

Bi-directional cranial X-ray of an individual who tried to commit suicide with a crossbow.

Improving X-ray imaging: the CAT scanner

History

- Röntgen, Hounsfield and Cormack
- 1967: first CAT scan
- 1972: prototype
- 1974: first clinical CAT image (head)
- 1976: whole body CAT scan
- 1979: Nobel-prize
- 1990: spiral CAT scanner
- 1992: multislice CAT scanner
- 2006: 64 slice (and more…)
- multiple and hybrid modes: SPECT-CT, PET-CT, Dual-source CT

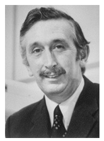

Godfrey Hounsfield

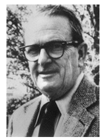

Allan Cormack

First, lab CT of a brain slice

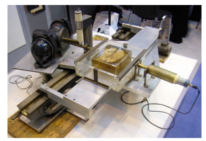

Prototype CAT scanner (EMI)

„Siretom" head scanner (1974)

128x128 pixel image (1975)

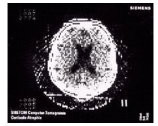

Multi-modal (combined) images

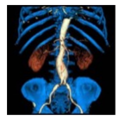

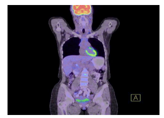

Summary

- **Tomographic** digital imaging method that uses **x-rays:** displays x-ray **absorbance** by the different points of the tomographic slice.
- **Multidetector** spiral CT (4-64 detector array): one slice 0.4-1 s; entire examination 5-15 s.
- **Ionizing** radiation. Absorbed **dose** ~50-100 times that of conventional x-ray. Significant **scattered** intensity.

Current CAT scanner

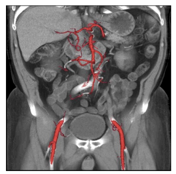

CT Foundations I: determination of μ

Objective: to determine the attenuation coefficient (μ_x) of the individual volume elements (voxels)

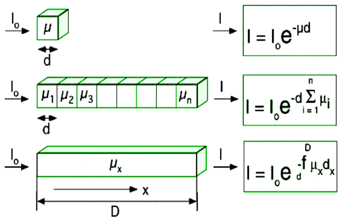

μ_x: linear attenuation coefficient
d_x: size of the voxel

CT Image: density matrix

$$N_{CT} = 1000 \frac{\mu - \mu_w}{\mu_w}$$

N_{CT}: density, CT number, Hounsfield units
μ: attenuation coefficient of voxel
μ_w: attenuation coefficient of water

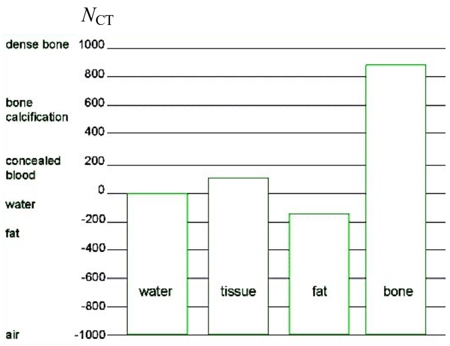

CT foundations II. scanninc

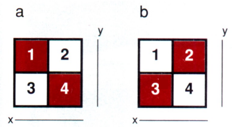

Problem: It is not possible to distinguish **a** from **b** in a bi-directional image

Solution: transaxial scanning along as large angular resolution as possible.

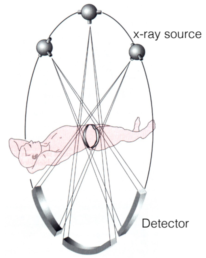

Conventional CT slice

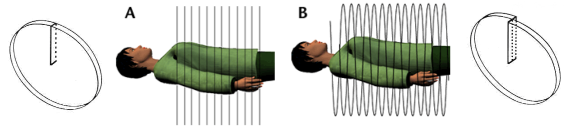

Spiral CT slice

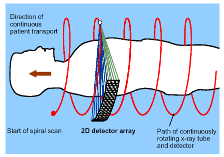

Multi-detector CT (MDCT)

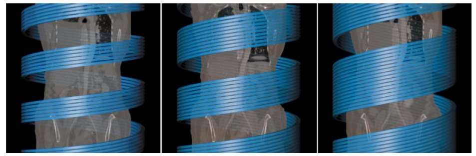

Multi-slice CT (MSCT)

CT foundations III: Image Reconstruction

1. Algebraic reconstruction techniques
2. Direct Fourier reconstruction
3. „Filtered Back Projection" (current method)

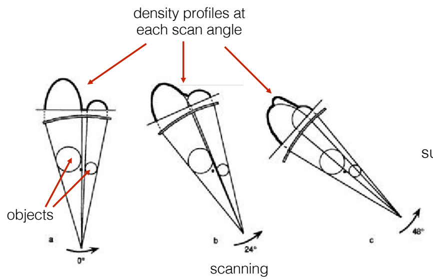

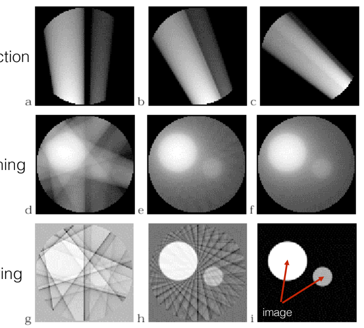

CT foundations IV: Contrast manipulation „Windowing"

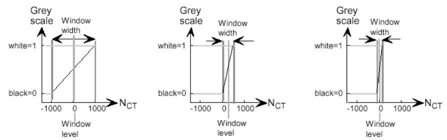

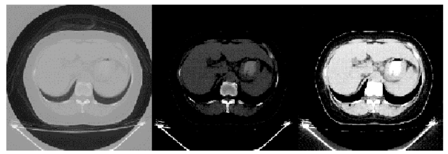

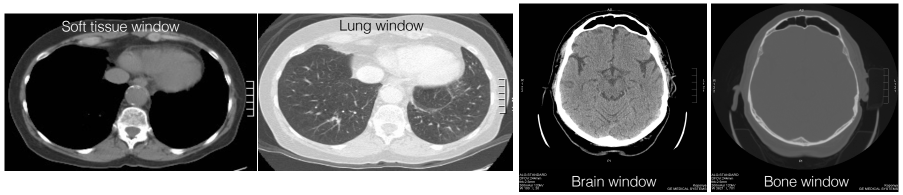

Modern CAT scanning

3D reconstruction, Virtual endoscopy

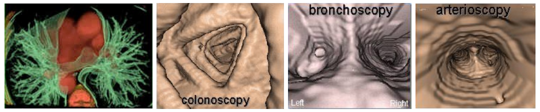

Increasing speed and resolution

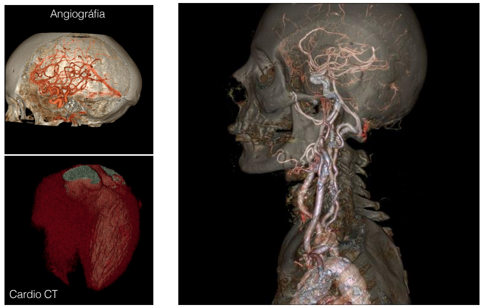

Combination with other modalities

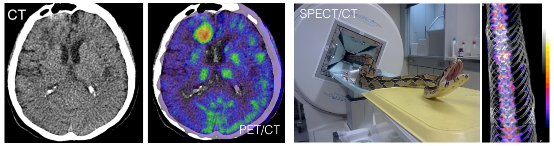

Photon Counting CT (PCCT)

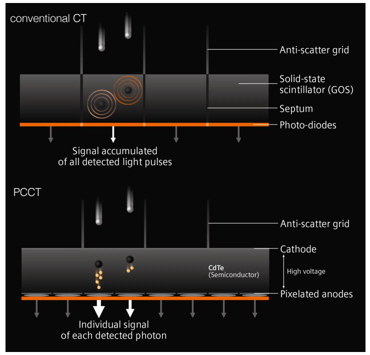

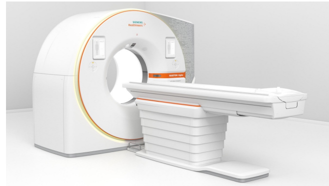

- PCD: Photon Counting Detector (cadmium telluride crystal, CdTe)
- PCD keeps track of the energy of incoming photons
- PCD provides x-ray energy spectrum
- increased sensitivity (lower x-ray dose, lower contrast-agent dose)
- functional imaging possibility

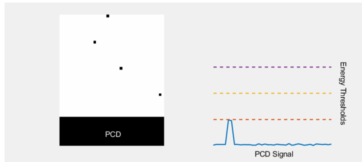

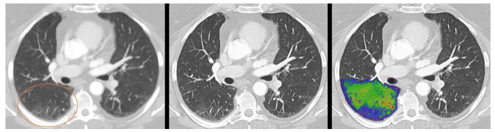

conventional CT | PCCT (increased detail) | PCCT (superimposed functional information)

Application II. Absorptiometry

Dual-energy X-ray absorptiometry (DXA or DEXA)

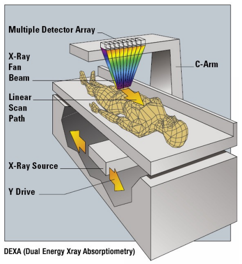

- Most important method for measuring bone density
- Characteristic X-ray is used as source
- Two different photon energies are employed (so that bone vs. soft-tissue absorption can be differentiated)
- Low dose is applied
- Whole-body scan is recorded
- Densities of distinct areas (e.g., femur, spine) are compared with reference databases
- Bone Mineral Density (BMD) calculated
- T-score is established

T-score: number of standard deviations below the average for a young adult at peak bone density.

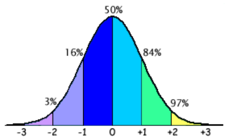

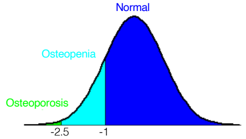

femur region | lumbar spine

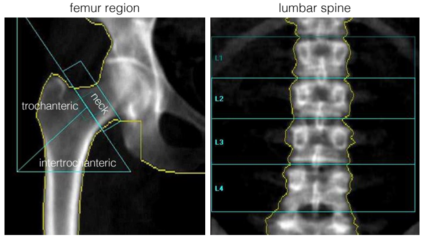

Application III. Radiation therapy

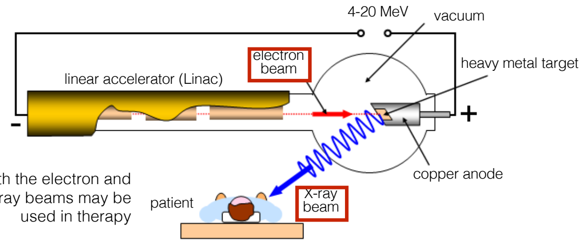

Both the electron and X-ray beams may be used in therapy

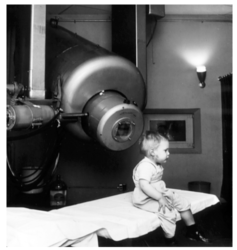

First patient (Gordon Isaacs) treated with Linac radiation therapy (electron beam) for retinoblastoma (1955)

Modern hospital Linac

Advantages:

- Radiation may be turned on and off
- No contaminating radioactivity

Generating high-energy X-ray

Linear accelerator (Linac)

- Charged particle (electron, proton) accelerated between electrodes (but not inside the electrode).
- Velocity of particle increases in steps.
- Electrode polarity is alternating.
- Electrodes are gradually longer (l_n increases) in order to maintain synchrony.
- Accelerated particles are directed at suitable target material (to generate X-ray).

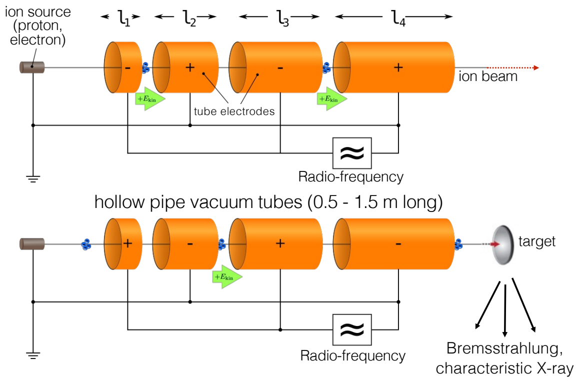

Ring-shape particle accelerators

Cyclotron

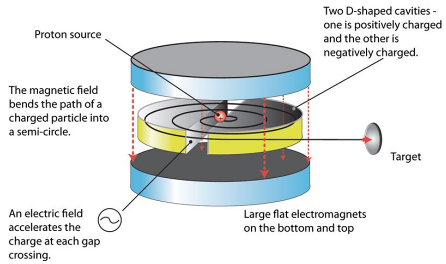

- Lorentz forces keep particles on circular path (causes limitations)
- Few tens of MeV particles are generated
- Used for generating positron-emitting isotopes (PET)
- Clinical cyclotrons in PET centers

11 MeV medical cyclotron

Synchrotron

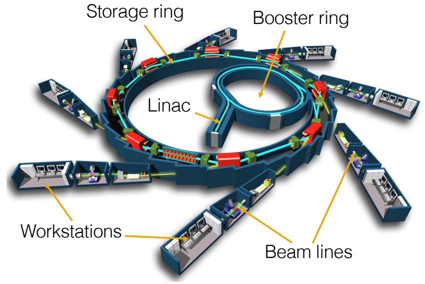

- Very high energy particles can be generated (GeV)
- Relativistic speeds can be achieved (near light speed)
- X-rays used for high-resolution structural research
- Few facilities around the world (Grenoble, Chicago, etc.)

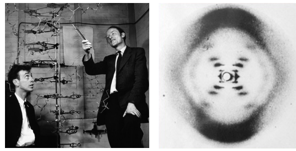

J.D. Watson and C.F. Crick, and the first x-ray image of DNA (1953)

Feedback

https://feedback.semmelweis.hu/feedback/pre-show-qr.php?type=feedback&qr=9X6WOHHVJG85SRFT